356 *Biochemistry* **2010,** *49,* 356–364
DOI: 10.1021/bi901681v

BIOCHEMISTRY
including biophysical chemistry & molecular biology
Article

Role of Signature Lysines in the Deviant Walker A Motifs of the ArsA ATPase[†]

Hsueh-Liang Fu,[‡] A. Abdul Ajees,[§] Barry P. Rosen,[§] and Hiranmoy Bhattacharjee*[,§]

[‡]*Department of Biochemistry and Molecular Biology, Wayne State University School of Medicine, Detroit, Michigan 48201 and* [§]*Department of Cellular Biology and Pharmacology, Herbert Wertheim College of Medicine, Florida International University, Miami, Florida 33199*

Received September 25, 2009; Revised Manuscript Received December 2, 2009

ABSTRACT: The ArsA ATPase belongs to the P-loop GTPase subgroup within the GTPase superfamily of proteins. Members of this subgroup have a deviant Walker A motif which contains a signature lysine that is predicted to make intermonomer contact with the bound nucleotides and to play a role in ATP hydrolysis. ArsA has two signature lysines located at positions 16 and 335. The role of Lys16 in the A1 half and Lys335 in the A2 half was investigated by altering the lysines individually to alanine, arginine, leucine, methionine, glutamate, and glutamine by site-directed mutagenesis. While Lys16 mutants show similar resistance phenotypes as the wild type, the Lys335 mutants are sensitive to higher concentrations of arsenite. K16Q ArsA shows 70% of wild-type ATPase activity while K335Q ArsA is inactive. ArsA is activated by binding of Sb(III), and both wild-type and mutant ArsAs bind Sb(III) with a 1:1 stoichiometry. Although each ArsA binds nucleotide, the binding affinity decreases in the order wild type > K16Q > K335Q. The results of limited trypsin digestion analysis indicate that both wild type and K16Q adopt a similar conformation during activated catalysis, whereas K335Q adopts a conformation that is resistant to trypsin cleavage. These biochemical data along with structural modeling suggest that, although Lys16 is not critical for ATPase activity, Lys335 is involved in intersubunit interaction and activation of ATPase activity in both halves of the protein. Taken together, the results indicate that Lys16 and Lys335, located in the A1 and A2 halves of the protein, have different roles in ArsA catalysis, consistent with our proposal that the nucleotide binding domains in these two halves are functionally nonequivalent.

The ArsAB pump in *Escherichia coli*, encoded by the *ars* operon of plasmid R773, confers resistance to arsenicals and antimonials. ArsA is the catalytic subunit of the pump that hydrolyzes ATP in the presence of arsenite [As(III)] or antimonite [Sb(III)]. ATP hydrolysis is coupled to extrusion of As(III) or Sb(III) through ArsB, which serves both as a membrane anchor for ArsA and as the substrate-conducting pathway (*1*). When expressed from a multicopy plasmid, the majority of ArsA is soluble in the cytosol, which allows large-scale purification and characterization. Purified ArsA exhibits low, basal level ATPase activity in the absence of metalloid and is activated by As(III) or Sb(III) (*2*).

ArsA is composed of homologous N-terminal (A1)[1] and C-terminal (A2) halves that are most likely the result of an ancestral gene duplication and fusion (*3*). Each half has a consensus Walker A motif or P-loop (*4*, *5*), which interacts with the phosphate moiety of ATP (*6*). In ArsA, the P-loop sequences are G_{15}KGGVGKT and G_{334}KGGVGKT in A1 and A2, respectively. This sequence differs from the classical Walker A motif in that it contains a "signature" lysine residue (Lys16 and Lys335) near the N-terminal end, and ArsA has been classified in the "deviant" Walker A motif subgroup (*7*).

More recently, ArsA has been assigned to the P-loop GTPase subgroup within the GTPase superfamily of proteins (*8*). Proteins containing the deviant Walker A motif have diverse functions, such as the iron protein NifH involved in nitrogen fixation, the plasmid and chromosome partitioning proteins ParA and Soj, respectively, the bacterial cell division regulator MinD, and the flagellar regulatory protein FleN (*7*, *9*).

Crystal structures have been obtained for four members of the deviant Walker A subfamily: ArsA (*6*), MinD (*10*−*12*), NifH (*13*−*15*), and Soj (*16*). Although the proteins differ considerably in their primary sequence, with ∼20% identity among them, their tertiary structures are largely superimposable (Figure 1). A DALI structural similarity comparison (*17*) of ArsA (PDB entry 1F48) with MinD (PDB entry 1G3Q), NifH (PDB entry 1N2C), and Soj (PDB entry 2BEK) yields *Z*-scores of 13.3, 12.7, and 12.1, respectively. What is the role of the signature lysine that is conserved in these structurally similar but functionally diverse proteins?

NifH is a dimer of identical subunits that are covalently linked by a 4Fe:4S cluster (*14*). When crystallized in the presence of ADP and AlF_4^- and as a complex with molybdenum iron (MoFe) protein, each of the two subunits of NifH rotates toward their nucleotide-bound interfaces forming a more compact dimer. In this transition state, the amino group of the signature lysine (Lys10) is 2.77 Å coordination distance with the terminal oxygen of the β-phosphate of ADP·AlF_4^- bound by the adjacent monomer. This signature lysine compensates for the negative charges of the bound nucleotide and is likely to be involved in the activation of ATPase activity (*9*).

[†]This study was supported by National Institutes of Health Grant GM55425.

*To whom correspondence should be addressed. Tel: (305) 348-1489. Fax: (305) 348-0651. E-mail: hbhatta@fiu.edu.

[1]Abbreviations: A1, N-terminal half of ArsA; A2, C-terminal half of ArsA; IPTG, isopropyl β-D-thiogalactoside; MOPS, 4-morpholinepropanesulfonic acid; MBD, metalloid binding domain; NBD, nucleotide binding domain; STD, signal transduction domain; SDS−PAGE, sodium dodecyl sulfate−polyacrylamide gel electrophoresis.

 Published on Web 12/10/2009

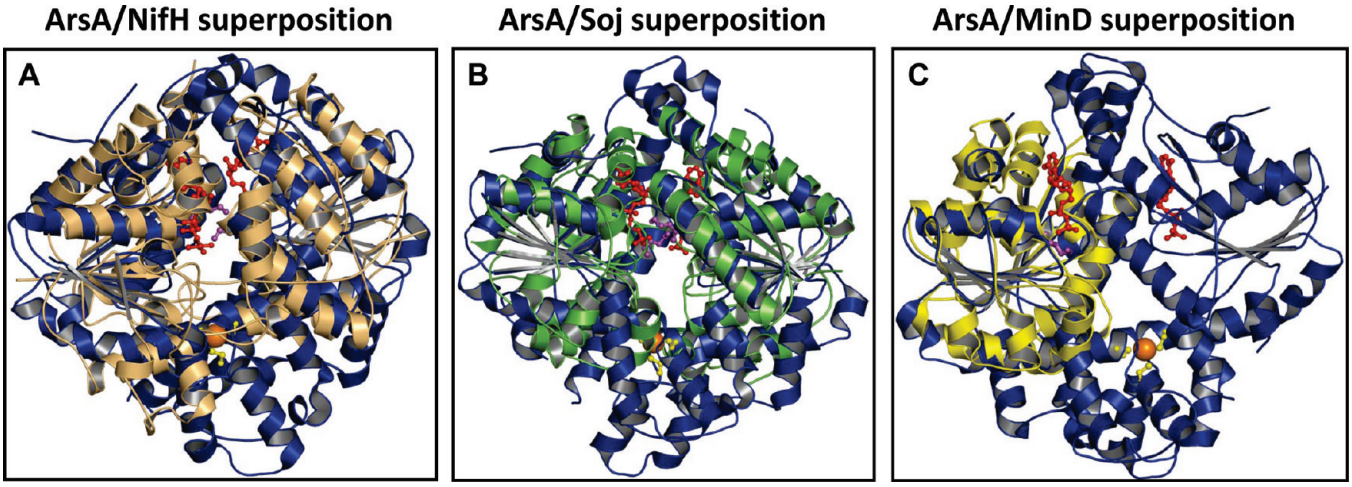

FIGURE 1: Comparison of the structures of ArsA, NifH, Soj, and MinD. (A) Structure of ArsA (blue) (PDB entry 1F48) superimposed on the structure of NifH (light orange) (PDB entry 1N2C), (B) Soj (green) (PDB entry 2BEK), and (C) MinD (yellow) (PDB entry 1G3Q). The bound nucleotides are in red, and the signature lysines are in magenta. Sb(III) bound to ArsA is shown as an orange sphere. Note that MinD has been crystallized only as a monomer and was superimposed on the A1 half of ArsA. NifH, Soj, and MinD were superimposed on ArsA using the program COOT (*35*), and the figures were rendered using PYMOL (http://www.pymol.org).

Soj exists as a monomer either in the absence of nucleotide or in the presence of ADP but undergoes ATP-dependent dimerization in solution (*16*). The hydrolysis-deficient mutant of Soj, Soj D44A, crystallizes as a dimer in the ATP-bound state that is structurally homologous to the NifH dimer. In this structure, the amino group of the signature lysine (Lys15) is in 2.96 Å coordination distance to the α-phosphate and 2.76 Å from the γ-phosphate of the ATP moiety bound by the adjacent chain. The ATP-dependent dimerization of Soj regulates its interaction with the DNA binding partner protein, Spo0J (*16*).

MinD crystallizes as a monomer (*10*−*12*) but undergoes ATP-dependent dimerization (*18*). MinD dimerization regulates its interaction with MinC/MinE, which is critical for the spatial regulation of cell division. Conformational changes upon binding ATP have been suggested to bring the signature lysine in each monomer closer to the other monomer, allowing formation of intermolecular lysine−nucleotide contacts (*9*).

ArsA is twice the size of homologues MinD, NifH, or Soj but is a pseudodimer consisting of two homologous domains, each similar to the monomeric homologues, that are connected by a short linker. Thus it contains two different signature lysine residues, Lys16 in the A1 half and Lys335 in the A2 half, unlike its homologues, which contain the same signature lysine in each monomer. ArsA has been crystallized with ADP bound to each nucleotide binding domain (NBD) (*6*). The adenine nucleotides bound at the two NBDs are stabilized by both polar and hydrophobic interactions reaching across the two halves of ArsA. For example, the hydroxyls of Thr501 and Thr502 from A2 form hydrogen bonds respectively with the ribose 3′-OH and with the β-phosphate oxygen of the ADP bound in the NBD1. However, Ser210 of NBD2, equivalent to Thr502 of the NBD1, is >6 Å away from the β-phosphate of ADP. This difference reflects that NBD2 is in a more open conformation than NBD1. Crystallization of ArsA in the presence of ATP led to occupancy of ATP at NBD2, while NBD1 contained only ADP (*19*). When ArsA crystals were incubated with the nonhydrolyzable analogue AMP-PNP, it was possible to exchange the nucleotide at NBD2, but not at NBD1, which suggests that NBD1 is in a closed conformation and is a high-affinity, poorly exchangeable site. In contrast, NBD2 is in an open conformation, with low affinity for nucleotide and is an easily exchangeable site. Structures of ArsA in the presence of ADP and AlF_3 were also determined with ADP in NBD1 and ADP·AlF_3 in NBD2 (*19*). In each structure, the signature lysines are >8 Å away from the nucleotides, too far to form intermonomer contacts. The objective of this study was to elucidate the individual roles of the two signature lysines, Lys16 in NBD1 and Lys335 in NBD2, in ArsA catalysis.

MATERIALS AND METHODS

Chemicals. 8-Azido[γ-^{32}P]ATP (15−20 Ci/mmol) was purchased from Affinity Labeling Technologies (Lexington, KY). Restriction grade thrombin was purchased from EMD Biosciences. Unless otherwise mentioned, all other chemicals were obtained from Sigma.

Media and Growth Conditions. *E. coli* cells were grown in Luria−Bertani medium (*20*) at 37 °C. Ampicillin (125 μg/mL), tetracycline (12.5 μg/mL), and isopropyl β-D-thiogalactoside (IPTG) (0.1 mM) were added as required. For arsenite resistance assays, overnight cultures of *E. coli* strain JM109 bearing wild-type and mutant *ars* plasmids were diluted 100-fold into fresh LB medium containing the indicated concentrations of sodium arsenite. After 6 h of growth at 37 °C, the absorbance at 600 nm was measured.

Oligonucleotide-Directed Mutagenesis. Mutations in *arsA* were introduced by site-directed mutagenesis using the QuikChange site-directed mutagenesis procedure (Stratagene). Plasmid pABH6 (*21*) containing wild-type *arsA* and *arsB* genes was used as the template to produce *arsA* mutants with various substitutions at Lys16 and Lys335. The mutagenic oligonucleotides used for both strands and the respective changes introduced (underlined) were as follows: K16A, G TTT TTT ACG GGT GCA GGA GGC GTG GGT AAA AC and GT TTT ACC CAC GCC TCC TGC ACC CGT AAA AAA C; K16E, G TTT TTT ACG GGT GAA GGA GGC GTG GGT AAA AC and GT TTT ACC CAC GCC TCC TTC ACC CGT AAA AAA C; K16L, G TTT TTT ACG GGT TTA GGA GGC GTG GGT AAA AC and GT TTT ACC CAC GCC TCC TAA ACC CGT AAA AAA C; K16M, G TTT TTT ACG GGT ATG GGA GGC GTG GGT AAA AC and GT TTT ACC CAC GCC TCC

CAT ACC CGT AAA AAA C; K16Q, G TTT TTT ACG GGT CAA GGA GGC GTG GGT AAA AC and GT TTT ACC CAC GCC TCC TTG ACC CGT AAA AAA C; K16R, G TTT TTT ACG GGT AGA GGA GGC GTG GGT AAA AC and GT TTT ACC CAC GCC TCC TCT ACC CGT AAA AAA C; K335A, CTG ATT ATG CTG ATG GGT GCA GGT GGC GTG GGG AAA AC and GT TTT CCC CAC GCC ACC TGC ACC CAT CAG CAT AAT CAG; K335E, G ATT ATG CTG ATG GGT GAA GGT GGC GTG GGG and CCC CAC GCC ACC TTC ACC CAT CAG CAT AAT C; K335L, G ATT ATG CTG ATG GGT TTA GGT GGC GTG GGG and CCC CAC GCC ACC TAA ACC CAT CAG CAT AAT C; K335M, G ATT ATG CTG ATG GGT ATG GGT GGC GTG GGG and CCC CAC GCC ACC CAT ACC CAT CAG CAT AAT C; K335Q, G ATT ATG CTG ATG GGT CAA GGT GGC GTG GGG and CCC CAC GCC ACC TTG ACC CAT CAG CAT AAT C; and K335R, G ATT ATG CTG ATG GGT AGA GGT GGC GTG GGG and CCC CAC GCC ACC TCT ACC CAT CAG CAT AAT C. Plasmid Th*arsA* (*22*), which contains the sequence for a thrombin enzyme cleavage site in the linker region connecting the two halves of ArsA, was used as the template to produce K16Q and K335Q Th*arsA* mutants.

DNA Manipulation and Sequence Analysis. Plasmid DNA was purified using the QIAprep spin miniprep kit (Qiagen). DNA ligation and transformation were performed as described (*20*, *23*). All mutations were confirmed by sequencing the entire gene using a CEQ2000 DNA sequencer (Beckman Coulter).

Purification of $[His]_6$*-Tagged ArsA ATPases*. Wild-type or mutant ArsA was purified from cultures of *E. coli* strain JM109 harboring either the wild-type or *tharsA* plasmids. Cells were grown at 37 °C in Luria−Bertani medium to an OD_{600} of 0.6, at which point 0.1 mM IPTG was added to induce ArsA expression. The cells were grown for another 3 h before being harvested by centrifugation. The soluble ArsA proteins were purified as described earlier (*21*). The concentration of ArsA in purified preparations was determined from the absorption at 280 nm using an extinction coefficient of 33480 M^{-1} cm^{-1} (*2*). ATPase activity was assayed using an NADH-coupled assay method (*24*).

Measurement of Metalloid Binding. Purified ArsA preparation was buffer-exchanged with 50 mM MOPS−KOH (pH 7.5) (buffer A) using a Micro Bio-Spin 6 column (Bio-Rad). The protein was incubated on ice with 2 mM ATPγS, 2.5 mM $MgCl_2$, and indicated concentrations of potassium antimonyl tartrate. After 1 h, each sample was passed through a Micro Bio-Spin 6 column, equilibrated with buffer A. Portions (25 μL) of the eluate were diluted with 2% HNO_3, and the metalloid content in the eluate was measured by inductively coupled mass spectrometry (ICP-MS), with a Perkin-Elmer ELAN 9000. Antimony standard solution was purchased from Ultra Scientific (North Kingstown, RI).

Labeling and Separation of A1 and A2 Halves of ArsA. Either ThArsA or the mutants (0.5 mg/mL) in buffer A containing 2.5 mM $MgCl_2$ and 0.25 mM EDTA were incubated in the dark at 4 or 37 °C for 10 min with 8-azido[γ-^{32}P]ATP (10 μCi/nmol) in the presence of 0.1 mM Sb(III). Routinely, 10 μM 8-azido[γ-^{32}P]ATP was used. However, for affinity measurements ArsA was incubated with increasing concentrations of 8-azido[γ-^{32}P]ATP, up to a maximum concentration of 50 μM. The samples were cross-linked by irradiation with a UV lamp (365 nm) for 10 min at 4 °C. The labeled proteins were incubated at room temperature for 3 h in the presence of 2.5 mM $CaCl_2$ and 1 unit of thrombin. Following proteolysis, the two halves of ArsA were separated by SDS−PAGE on 12% acrylamide gels. Gels were dried and exposed to Bio-Max MR film (Eastman Kodak Co.) at −70 °C for 12−24 h. The radioactivity incorporated into the ArsA band was quantified using a Cyclone Plus storage phosphor system (PerkinElmer) and OptiQuant software. The data were analyzed using SigmaPlot 11.0.

Limited Trypsin Digestion of ArsA. Limited trypsin digestion was performed at room temperature in buffer A containing 0.25 mM EDTA and 1 mg/mL ArsA. The ArsA:trypsin ratio was 500:1 (w/w). ArsAs were incubated with 5 mM ATP, 5 mM Mg^{2+}, and 0.5 mM Sb(III) either alone or in different combinations. Digestion was initiated by the addition of *N*-*p*-tosyl-L-phenylalanine chloromethyl ketone-treated trypsin (Sigma). Proteolysis was terminated at the indicated times by addition of a 10-fold excess of soybean trypsin inhibitor to the reaction mixture (*25*). Samples were analyzed by 12% SDS−PAGE and Coomassie Blue staining. The band intensity of either the 63-kDa full-length or 50-kDa truncated ArsA in each lane was quantitated using the UN-SCAN-IT gel analysis software (Silk Scientific).

RESULTS

Effect of Alteration of Lys16 and Lys335 on Metalloid Resistance. Lys16 and Lys335 in ArsA were individually changed to alanine, glutamate, leucine, methionine, glutamine, and arginine by site-directed mutagenesis. Cells bearing the mutated *arsA* and wild-type *arsB* genes were characterized phenotypically for arsenite resistance. Cells expressing wild-type *arsA* and *arsB* genes could grow in medium containing 5 mM sodium arsenite, cells without an *ars* operon were sensitive at 1 mM sodium arsenite, while cells expressing *arsB* alone were slightly more resistant than the vector alone control (Figure 2). Replacement of Lys16 with various amino acids did not significantly alter arsenite resistance compared to the wild type (Figure 2A). In contrast, alterations at Lys335 resulted in phenotypes intermediate between sensitive and fully resistant cells (Figure 2B). These results suggest that Lys335 but not Lys16 is involved in resistance.

Expression and Cellular Location of Altered ArsAs. The steady-state level of wild-type and altered ArsAs in cells was estimated by immunoblot analysis using antiserum to wild-type ArsA. Each altered protein was produced in approximately the same amount and migrated with the same mobility as wild-type ArsA (data not shown). Although ArsA is functionally a component of the membrane-bound pump, it is found in the cytosol when highly expressed (*2*). Each of the altered ArsAs was found predominantly in the cytosol at similar levels as the wild type (data not shown). Thus the mutations do not appear to affect synthesis or overall folding of the protein. Further biochemical characterizations were done only with K16Q and K335Q ArsA.

Properties of K16Q and K335Q ArsA. Wild-type, K16Q, and K335Q ArsAs were purified by Ni^{2+} affinity chromatography to >95% homogeneity, as described under Materials and Methods. The altered ArsAs were analyzed for their ability to hydrolyze ATP. In the presence of 5 mM ATP, 2.5 mM $MgCl_2$, and 0.1 mM potassium antimonial tartrate, wild-type ArsA exhibited a V_{max} of 800 nmol of ATP hydrolyzed min^{-1} (mg of protein)$^{-1}$. K16Q exhibited approximately 70% of wild-type activity, but K335Q was inactive. The K_m for ATP increased

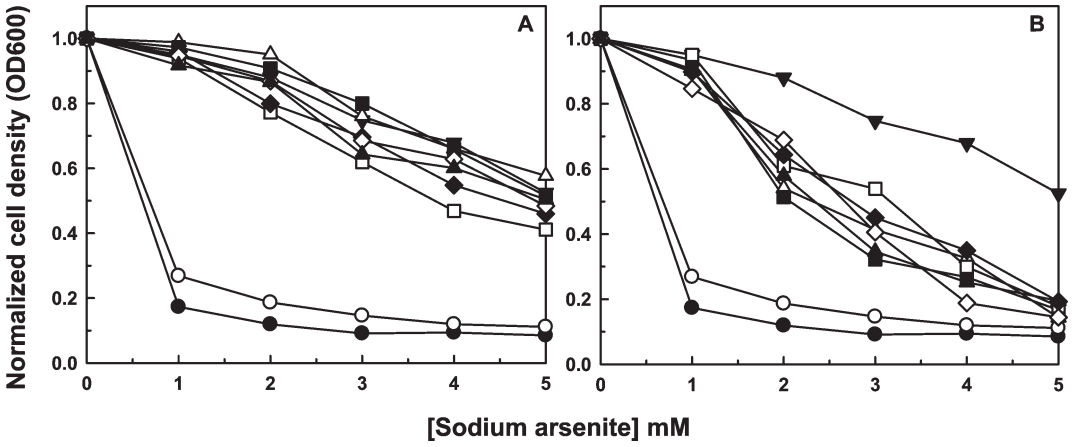

FIGURE 2: Resistance to arsenite in cells expressing wild-type and altered ArsA. Overnight cultures of *E. coli* strain JM109 bearing wild-type and mutant *ars* plasmids were diluted 100-fold into fresh Luria−Bertani medium containing the indicated concentrations of sodium arsenite. Expression of the *ars* genes was induced with 0.1 mM IPTG. After 5 h of growth at 37 °C, the optical density at 600 nm was measured. Cells contained the following plasmids: panel A, (▼) pABH6 (*arsAB*), (△) pK16A ($arsA_{K16A}B$), (■) pK16E ($arsA_{K16E}B$), (□) pK16L ($arsA_{K16L}B$), (◆) pK16M ($arsA_{K16M}B$), (◇) pK16Q ($arsA_{K16Q}B$), (▲) pK16R ($arsA_{K16R}B$), (○) pALTER-B (*arsB*), and (●) vector plasmid pALTER-1; panel B, (▼) pABH6 (*arsAB*), (△) pK335A ($arsA_{K335A}B$), (■) pK335E ($arsA_{K335E}B$), (□) pK335L ($arsA_{K335L}B$), (◆) pK335M ($arsA_{K335M}B$), (◇) pK335Q ($arsA_{K335Q}B$), (▲) pK335R ($arsA_{K335R}B$), (○) pALTER-B (*arsB*), and (●) vector plasmid pALTER-1.

from 0.17 mM for the wild type to 0.52 mM for K16Q. The concentration of antimonite required for half-maximal activation was determined to be 20 μM for K16Q, which is 10-fold higher than the wild type. Thus Lys16 is not required for activity. Since replacement of Lys335 results in loss of activity, this residue is more likely to be involved in catalysis. Since purified K335Q ArsA exhibits no ATP hydrolysis, why do cells expressing this protein show intermediate growth in the presence of As(III)? One possibility is that K335Q ArsA has labile ATPase activity that is rapidly lost during purification. Since the protein is constantly synthesized *in vivo*, even labile activity would confer some resistance.

Effect of Lysine Substitutions on Metalloid Binding. The ability of mutant ArsAs to bind Sb(III) was measured by rapid gel filtration. Binding to purified ArsA was measured as a function of Sb(III) concentration. In the presence of saturating MgATPγS, metalloid binding to wild-type ArsA was saturable, with a stoichiometry of one Sb(III) per wild-type ArsA (Figure 3). As reported previously, Sb(III) is bound to A1 residue Cys113 and A2 residue Cys422 (*26*). Both K16Q and K335Q bound Sb(III) in a 1:1 ratio, while the C113A/C422A derivative bound only background levels of Sb(III) (Figure 3). These results indicate that alteration of either Lys16 or Lys335 does not affect metalloid binding to ArsA. The direct binding assay does not provide data that are sufficiently accurate for estimating metalloid affinity, as the concentration of ArsA used in the experiment (10 μM) was near the apparent K_d for Sb(III).

Effect of Lysine Substitutions on Nucleotide Binding. To investigate the effect of lysine mutations on nucleotide binding in either A1 or A2, a derivative, ThArsA, in which a thrombin enzyme cleavage site had been introduced into the linker region that connects the two halves of ArsA (*22*) was used as a template to create the substitutions. Thrombin cleavage results in the generation of a 34-kDa A1 fragment and a smaller A2 fragment. Lys16 and Lys335 in ThArsA were individually altered to glutamine to create the K16Q and K335Q ThArsA mutants. There was little difference between the arsenite resistance conferred by wild-type *arsA* and the *tharsA* gene. Similarly, cells expressing K16Q or K335Q *tharsA* showed phenotypes nearly identical to those of the K16Q or K335Q mutants (data not shown). Each of the ThArsA mutants was purified to >95% homogeneity by Ni^{2+} affinity chromatography and analyzed for ArsA activity.

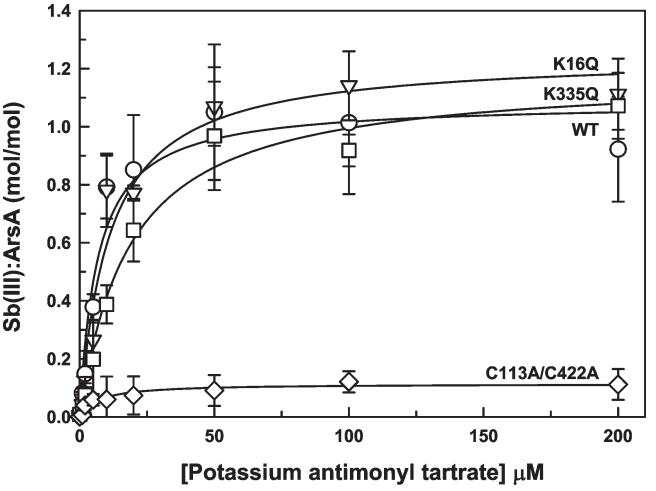

FIGURE 3: Stoichiometry of Sb(III) binding to wild-type and altered ArsA. Binding of Sb(III) to (○) wild type (WT), (▽) K16Q, (□) K335Q, and (◇) C113A/C422A was determined after incubating 10 μM ArsA with 2 mM ATPγS, 2.5 mM $MgCl_2$, and the indicated concentrations of potassium antimonyl tartrate. The lines represent the best fit of the data using SigmaPlot 11.0. The error bars represent standard deviations (n = 3).

Purified preparations of ThArsA consistently exhibited 75% of wild-type ATPase activity, slightly higher than reported earlier (*22*). The K_m for ATP was determined to be 0.17 mM, and the concentration of Sb(III) required for half-maximal activation of ThArsA was 2 μM, similar to the wild-type enzyme. K16Q ThArsA showed ~90% of ThArsA activity. The concentrations of ATP and Sb(III) required for half-maximal activation of K16Q ThArsA were 5-fold and 10-fold higher, respectively, than ThArsA. The K335Q ThArsA was inactive. These data indicate that K16Q and K335Q created in either wild-type or ThArsA backgrounds are sufficiently similar to merit azido-labeling experiments.

ThArsA derivatives were labeled with increasing concentrations of 8-azido[γ-^{32}P]ATP in the presence of 0.1 mM Sb(III) at

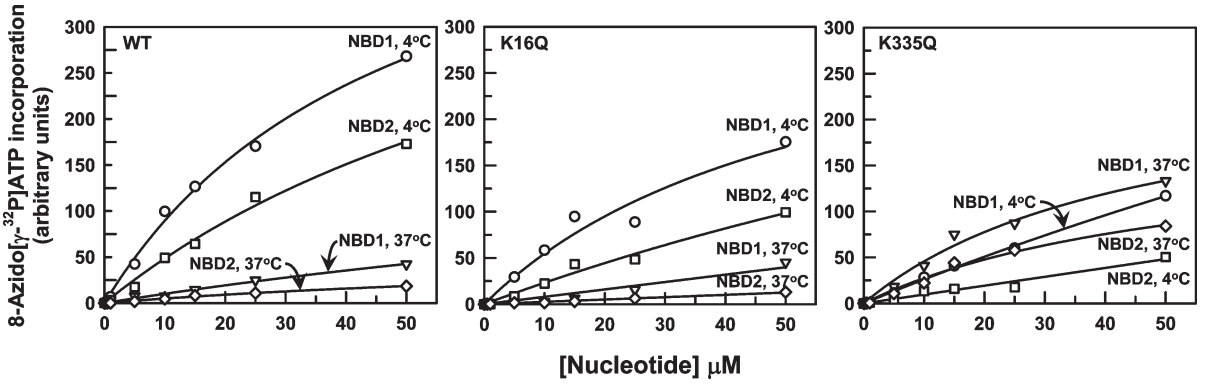

FIGURE 4: Binding of 8-azido[γ-^{32}P]ATP by NBD1 and NBD2 in wild-type and altered ArsA. ThArsA (25 μg) was incubated with increasing concentrations of 8-azido[γ-^{32}P]ATP at 4 or 37 °C in the presence of 0.1 mM potassium antimonyl tartrate [Sb(III)], photo-cross-linked, and digested with thrombin as described in Materials and Methods. Radioactivity incorporated into the NBD1 and NBD2 bands was quantified using a PhosphorImager and plotted as a function of the nucleotide concentration. The lines represent a nonlinear least-squares fit to a hyperbolic function. The experiment shown in this figure was repeated twice, and the data shown are representative of the results.

either 4 or 37 °C. This allows measurement of both binding and hydrolysis of nucleotide, respectively (*22*). Samples were digested with thrombin and separated by SDS−PAGE, and the autoradiographs were quantified by densitometry. At 4 °C, a condition that promotes binding but not catalysis, both NBDs of ThArsA were labeled with 8-azido[γ-^{32}P]ATP, although the amount of label incorporated into NBD1 was consistently greater than that in NBD2 (Figure 4). Binding to the two NBDs was measured as a function of nucleotide concentration. Binding to NBD1 was saturable with an apparent K_d of 50 μM, while NBD2 exhibited a 2-fold lower affinity than NBD1. At 37 °C, a condition that promotes catalysis, both NBDs of ThArsA showed considerably less labeling than at 4 °C, indicating hydrolysis of the trinucleotide and liberation of the γ-phosphate.

K16Q ThArsA also bound and hydrolyzed 8-azido-[γ-^{32}P]ATP, although the levels of nucleotide binding at either NBDs were slightly less than that of ThArsA (Figure 4). When compared to ThArsA, NBD1 showed a slight decrease in affinity for the nucleotide with an apparent K_d of 55 μM, while NBD2 exhibited a 4-fold lower affinity than NBD1. At 4 °C, K335Q ThArsA bound 8-azido[γ-^{32}P]ATP at both NBDs but at slightly lower levels than the K16Q enzyme (Figure 4). In comparison to ThArsA, NBD1 exhibited a 6-fold decrease in affinity for the nucleotide, while the apparent affinity at NBD2 was too low to quantify. Interestingly, the K335Q mutant did not show release of γ-^{32}P at 37 °C (Figure 4), consistent with its inability to hydrolyze ATP in steady-state assays. We interpret this finding as the inability of the K335Q mutant to assume an open conformation upon nucleotide binding and thus does not complete the catalytic cycle.

Effect of Lysine Substitutions on Accessibility to Trypsin. ArsA undergoes a number of conformational changes during the catalytic cycle (*27*−*31*). We have used accessibility to trypsin as an indicator of conformation (*25*, *26*, *32*). At least five conformations of the enzyme can be distinguished by limited trypsin digestion. In the absence of any ligands, where no catalysis occurs, the enzyme is in an open conformation, in which A1 and A2 are far enough apart to allow access to trypsin to the surface of each. In this open state, ArsA is extremely sensitive to trypsin digestion. Trypsin cleaves the ArsA at Arg290 to produce a 32-kDa A1 fragment that remains stable to trypsin digestion and a slightly smaller A2 fragment that is digested rapidly (*33*). A second less open conformation is observed in the presence of ATP alone (noncatalytic conditions), where the enzyme is rapidly degraded to a 50-kDa fragment, which is then slowly digested to a ~30-kDa species. The third conformation is also observed under noncatalytic conditions but in the presence of both ATP and metalloid. In this partially closed conformation, the rate of trypsin digestion is retarded, indicating that binding of both ATP and metalloid results in the formation of an interface between A1 and A2 that is not accessible to trypsin. This effect of nucleotide and metalloid together is synergistic in that neither alone produces this conformation. The fourth conformation is a more closed conformation, observed in the presence of MgATP, where the enzyme exhibits basal ATPase activity. In this conformation, the rate of trypsin digestion is even slower than under noncatalytic conditions, suggestive of formation of a different interface between A1 and A2. Finally, a fifth conformation is observed during metalloid-stimulated catalysis. In this state, ArsA becomes sensitized to trypsin again. The 63-kDa ArsA is cleaved to a 50-kDa species, which remains insensitive to trypsin digestion for a significant length of time, indicating a different conformation of ArsA during metalloid-stimulated activity. Our interpretation is that ArsA alternates between open and closed conformations during activated catalysis. Thus, part of the time trypsin is excluded from the A1−A2 interface, and part of the time the surface of A2 is accessible to trypsin.

As discussed above, in the absence of substrates, wild-type ArsA is rapidly cleaved by trypsin to one or more polypeptides of 30 kDa (*26*). Each lysine mutant exhibited a similar proteolytic pattern as the wild type in the absence of ligands (Figure 5A). Upon incubation of wild-type ArsA with ATP followed by treatment with trypsin, a 50-kDa species was first observed that was subsequently cleaved to smaller fragments (Figure 5A). Addition of ligands in various combinations had a dramatic effect on accessibility to trypsin, and the rates of proteolysis of the intact 63-kDa and 50-kDa species from the wild-type and K335Q proteins were quantitated by densitometry (Figure 5B). The K16Q was nearly identical to the wild type and is not shown in Figure 5B. In the presence of ATP, disappearance of both the wild type and K335Q 63-kDa bands followed an apparent first-order kinetics, with a $t_{1/2}$ of 15 and 16 min, respectively (Figure 5B), indicating that the altered proteins adopt a similar conformation as the wild type upon binding ATP. Incubation with Sb(III) alone afforded no protection from proteolysis to either the wild-type or altered proteins (Figure 5A). The rate of cleavage of wild-type ArsA was decreased synergistically when both ATP and Sb(III) were present (Figure 5A); the half-life of

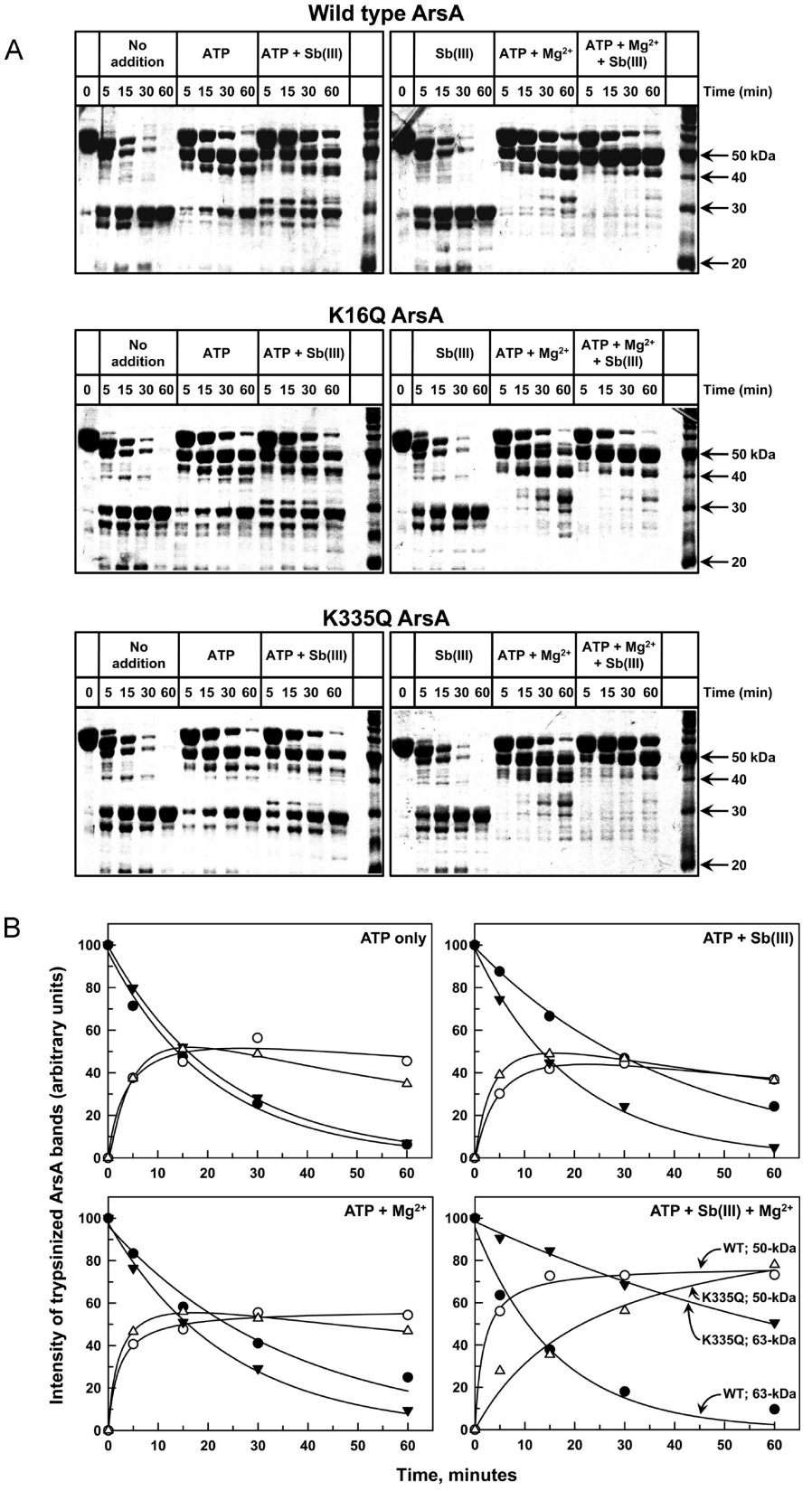

FIGURE 5: Effect of alteration of Lys16 or Lys335 on accessibility to trypsin. (A) Trypsin digestion was performed at room temperature with the indicated additions: 5 mM ATP, 0.5 mM potassium antimonyl tartrate [Sb(III)], or 5 mM $MgCl_2$. ArsA proteins were treated with trypsin as described in Materials and Methods. At the indicated times, samples were removed, and the reactions were terminated by the addition of soybean trypsin inhibitor. The tryptic products were analyzed by 12% SDS−PAGE and stained with Coomassie Blue. The positions of migration of standards are indicated. (B) Kinetics of limited trypsin digestion. The relative amounts of full-length (●, ▼) and 50-kDa species (○, △) of either the wild-type (●, ○) or K335Q (▼, △) ArsA were quantitated by densitometric scanning, expressed as a percent of the full-length ArsA at 0 min, and plotted as a function of time. The lines showing the degradation of the intact 63-kDa band represent a nonlinear least-squares fit to an exponential decay function. The lines showing the generation of the 50-kDa species represent a nonlinear least-squares fit to a hyperbolic function.

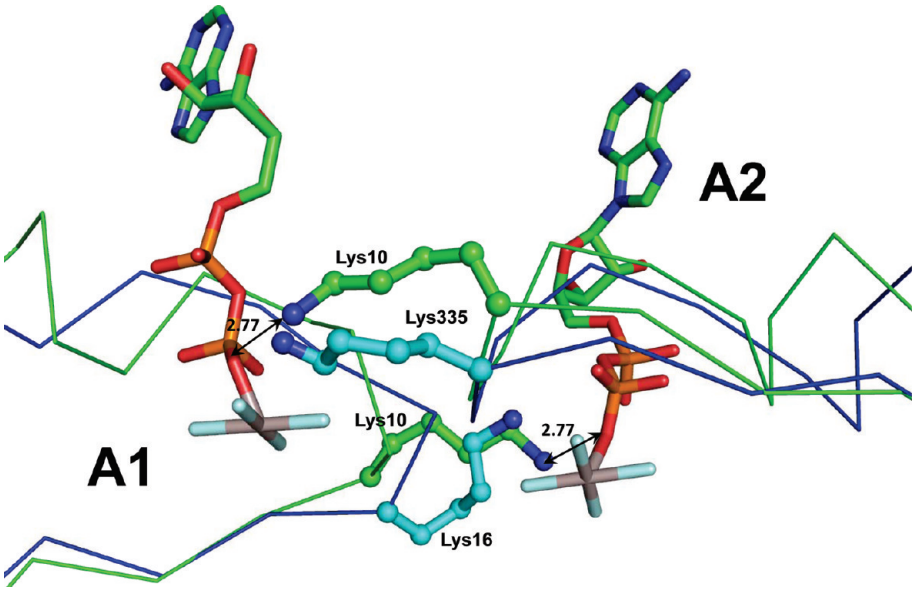

FIGURE 6: Model of the signature lysines in ArsA and NifH dimers. The cartoon depicts the A1 and A2 halves of ArsA (blue line) superimposed on a NifH dimer (green line). The NifH structure was obtained in the presence of ADP·AlF_4^- and MoFe protein. The MoFe protein and the 4Fe-4S cluster in NifH have been omitted for simplicity. ADP·AlF_4^- is shown as stick model and colored according to atom type (carbon, green; nitrogen, blue; oxygen, red; phosphorus, orange; and AlF_4^-, gray). The signature lysines are shown as ball and stick models. The carbon backbone of ArsA Lys16 and Lys335 is shown in cyan. The NifH signature Lys10 is shown in green. The amino nitrogens are shown in blue. The amino group of Lys10 is 2.77 Å from the β-phosphate of ADP. Lys16 and Lys335 of ArsA have been modeled to bring them to a similar distance to the β-phosphate of ADP of the opposing half of ArsA to represent the structure in its transition state.

limited proteolysis of the 63-kDa band increased to 28 min. In contrast, synergistic protection was not observed for K335Q ArsA; the half-life of disappearance of the 63-kDa form was 14 min, which is similar to that observed in the presence of ATP alone. Therefore, although K335Q binds Sb(III) (Figure 3), it adopts a more open, trypsin-accessible conformation even in the presence of ATP and Sb(III). Addition of Mg^{2+} alone had no effect on proteolysis (data not shown). In the presence of ATP and Mg^{2+}, conditions that produce basal hydrolysis, similar synergistic protection was observed for wild-type ArsA (Figure 5A). Full-length, wild-type 63-kDa ArsA was cleaved with a half-life of 25 min to a long-lived 50-kDa species in the presence of ATP and Mg^{2+} (Figure 5). Both K16Q and K335Q ArsAs showed a similar pattern of proteolysis as the wild type with those two ligands (Figure 5A), indicating that both wild type and mutants assume similar conformations during basal ATPase activity. Both of the altered proteins were slightly more sensitive to proteolysis than the wild type (Figure 5A); the half-lives of the reaction were 17 min for K335Q (Figure 5B) and 10 min for K16Q (not shown).

When all three ligands, ATP, Sb(III), and Mg^{2+}, were added together, conditions that produce activated catalysis, the 63-kDa wild-type ArsA was rapidly digested with a half-life of 11 min (Figure 5B) to a 50-kDa species, which was stable to further trypsin attack (Figure 5A). K16Q behaved similarly as the wild type, with rapid formation of the 50-kDa species (Figure 5A). In contrast, K335Q exhibited greater stability of the full-length protein (Figure 5A), with a half-life of >60 min for disappearance of the 63-kDa band and slower formation of the 50-kDa form (Figure 5B). Thus, K335Q acquires a closed conformation during metalloid-stimulated catalysis that is different from the open conformation of the wild type. In this closed conformation, the trypsin sites on the faces of A1 and A2 that form the interface between the two halves are quite inaccessible to the protease. Our interpretation is that the catalytically inactive K335Q mutant assumes an open conformation only very slowly under catalytic conditions. This implies that Lys335 (but not Lys16) is involved in formation of an open conformation during the catalytic cycle.

DISCUSSION

The roles of the signature lysines, Lys16 in A1 and Lys335 in A2, in ArsA catalysis were investigated by mutating the lysines to alanine, glutamate, leucine, methionine, glutamine, or arginine. Several lines of evidence indicate that the Lys16 or Lys335 substitutions did not affect the overall conformation. First, the altered proteins were produced in normal amounts and were not degraded *in vivo*. Second, each altered protein bound metalloid in the same 1:1 stoichiometry as wild type. Third, both wild type and altered ArsAs showed an overall similar trypsin digestion pattern under noncatalytic conditions.

Upon addition of MgATP, which allows for low-level basal ATPase activity, the two lysine mutants appeared to be more sensitive to trypsin cleavage than the wild type. This would indicate that the mutants adopt a more open conformation during basal catalysis, rendering them more accessible to protease than the wild type. In the presence of MgATP and Sb(III), a condition which produces activated ATP hydrolysis, did the K335Q exhibit a significant difference in sensitivity to trypsin proteolysis compared to either the wild-type or K16Q ArsA. Both wild type and K16Q were more accessible to trypsin under activated conditions than under basal conditions, consistent with our suggestion that the interface between A1 and A2 is alternatively accessible and inaccessible to trypsin during the catalytic cycle, i.e., the enzyme alternates between open and closed conformations. In contrast, K335Q adopted a more trypsin-resistant conformation under activated conditions, indicating that the interface between A1 and A2 in this mutant remains not as accessible as in the wild type. Thus, even though purified K335Q is inactive, it adopts a closed conformation in the presence of MgATP and Sb(III),

showing that it still binds its ligands even if it cannot undergo a full catalytic cycle at the same rate as the wild type. The mutant enzyme may undergo the next step in the catalytic cycle very slowly, indicating a critical role for Lys335.

The crystal structure of the NifH dimer in the presence of ADP and AlF_4^- reveals that the signature lysine in the deviant Walker A motif establishes intermonomer contact with the β-phosphate of the bound ADP·AlF_4^-. Is it possible that alteration of the signature lysines of ArsA lowers their affinity for nucleotide? While the K335Q was inactive, K16Q has a 3-fold reduction in the affinity of ATP and a 10-fold lower affinity for Sb(III). Azido-ATP labeling studies indicated that while both K16Q and K335Q bind nucleotide at both NBD1 and NBD2, the binding affinity decreases in the order wild-type > K16Q > K335Q. While K16Q hydrolyzes azidoATP at both NBD1 and NBD2, K335Q ArsA does not exhibit ATP hydrolysis at either site.

In the structure of NifH complexed with ADP (PDB entry 1FP6) the signature lysine (Lys15) is 8.5 Å from the β-phosphate of ADP. However, in the presence of ADP·AlF_4^- and its partner MoFe protein, each of the monomers of NifH rotates ~13° toward the subunit interface forming a more compact structure such that the signature lysines are now 2.77 Å from the β-phosphate. The ArsA structure (PDB entry 1F48) shows that the amino group of Lys16 is 8.38 Å from the β-phosphate of ADP at NBD2 and the amino group of Lys335 is 11.5 Å from the β-phosphate of ADP at NBD1. Based on the structure of NifH complexed with MoFe protein and the biochemical data presented above, we propose that ArsA undergoes conformational changes upon binding ATP, which brings the signature lysine close to ATP to form lysine−nucleotide contacts (Figure 6). Lys335 likely stabilizes the charge of the bound nucleotide at NBD1 and is consequently involved in activation of ATPase activity. Lys16 is slightly more distant than would be required to have a strong electrostatic interaction with the negative charge of the bound nucleotide at NBD2, and consequently, alteration of Lys16 has much less effect on ATPase activity. A similar phenomenon was observed with the conserved aspartates, Asp142 and Asp447, located in the A1 and A2 signal transduction domain, respectively (*34*). While alteration of Asp142 resulted in loss of Mg^{2+} binding to NBD1, Asp447 was found not to be nearly as critical for Mg^{2+} binding as Asp142. In summary, the results indicate that the two signature lysines, Lys16 and Lys335, have different roles in ArsA catalysis, supporting our hypothesis that NBD1 and NBD2 of the two halves of ArsA are functionally nonequivalent.

REFERENCES

1. Tisa, L. S., and Rosen, B. P. (1990) Molecular characterization of an anion pump. The ArsB protein is the membrane anchor for the ArsA protein. *J. Biol. Chem. 265*, 190–194.
2. Rosen, B. P., Weigel, U., Karkaria, C., and Gangola, P. (1988) Molecular characterization of an anion pump. The *arsA* gene product is an arsenite (antimonate)-stimulated ATPase. *J. Biol. Chem. 263*, 3067–3070.
3. Chen, C. M., Misra, T. K., Silver, S., and Rosen, B. P. (1986) Nucleotide sequence of the structural genes for an anion pump. The plasmid-encoded arsenical resistance operon. *J. Biol. Chem. 261*, 15030–15038.
4. Walker, J. E., Saraste, M., Runswick, M. J., and Gay, N. J. (1982) Distantly related sequences in the α- and β-subunits of ATP synthase, myosin, kinases and other ATP-requiring enzymes and a common nucleotide binding fold. *EMBO J. 1*, 945–951.
5. Bossemeyer, D. (1994) The glycine-rich sequence of protein kinases: a multifunctional element. *Trends Biochem. Sci. 19*, 201–205.
6. Zhou, T., Radaev, S., Rosen, B. P., and Gatti, D. L. (2000) Structure of the ArsA ATPase: the catalytic subunit of a heavy metal resistance pump. *EMBO J. 19*, 4838–4845.
7. Koonin, E. V. (1993) A superfamily of ATPases with diverse functions containing either classical or deviant ATP-binding motif. *J. Mol. Biol. 229*, 1165–1174.
8. Leipe, D. D., Wolf, Y. I., Koonin, E. V., and Aravind, L. (2002) Classification and evolution of P-loop GTPases and related ATPases. *J. Mol. Biol. 317*, 41–72.
9. Lutkenhaus, J., and Sundaramoorthy, M. (2003) MinD and role of the deviant Walker A motif, dimerization and membrane binding in oscillation. *Mol. Microbiol. 48*, 295–303.
10. Cordell, S. C., and Lowe, J. (2001) Crystal structure of the bacterial cell division regulator MinD. *FEBS Lett. 492*, 160–165.
11. Hayashi, I., Oyama, T., and Morikawa, K. (2001) Structural and functional studies of MinD ATPase: implications for the molecular recognition of the bacterial cell division apparatus. *EMBO J. 20*, 1819–1828.
12. Sakai, N., Yao, M., Itou, H., Watanabe, N., Yumoto, F., Tanokura, M., and Tanaka, I. (2001) The three-dimensional structure of septum site-determining protein MinD from *Pyrococcus horikoshii* OT3 in complex with Mg-ADP. *Structure 9*, 817–826.
13. Georgiadis, M. M., Komiya, H., P., C., Woo, D., Kornuc, J. J., and Rees, D. C. (1992) Crystallographic structure of the nitrogenase iron protein from *Azotobacter vinelandii*. *Science 257*, 1653–1659.
14. Schindelin, H., Kisker, C., Schlessman, J. L., Howard, J. B., and Rees, D. C. (1997) Structure of ADP·AIF_4^- stabilized nitrogenase complex and its implications for signal transduction. *Nature 387*, 370–376.
15. Tezcan, F. A., Kaiser, J. T., Mustafi, D., Walton, M. Y., Howard, J. B., and Rees, D. C. (2005) Nitrogenase complexes: multiple docking sites for a nucleotide switch protein. *Science 309*, 1377–1380.
16. Leonard, T. A., Butler, P. J., and Lowe, J. (2005) Bacterial chromosome segregation: structure and DNA binding of the Soj dimer—a conserved biological switch. *EMBO J. 24*, 270–282.
17. Holm, L., and Sander, C. (1995) Dali: a network tool for protein structure comparison. *Trends Biochem. Sci. 20*, 478–480.
18. Hu, Z., Saez, C., and Lutkenhaus, J. (2003) Recruitment of MinC, an inhibitor of Z-ring formation, to the membrane in *Escherichia coli*: role of MinD and MinE. *J. Bacteriol. 185*, 196–203.
19. Zhou, T., Radaev, S., Rosen, B. P., and Gatti, D. L. (2001) Conformational changes in four regions of the *Escherichia coli* ArsA ATPase link ATP hydrolysis to ion translocation. *J. Biol. Chem. 276*, 30414–30422.
20. Sambrook, J., and Russell, D. (2001) Molecular Cloning: A Laboratory Manual, 3rd ed., Cold Spring Harbor Laboratory Press, Cold Spring Harbor, NY.
21. Bhattacharjee, H., and Rosen, B. P. (2000) Role of conserved histidine residues in metalloactivation of the ArsA ATPase. *Biometals 13*, 281–288.
22. Jiang, Y., Bhattacharjee, H., Zhou, T., Rosen, B. P., Ambudkar, S. V., and Sauna, Z. E. (2005) Nonequivalence of the nucleotide binding domains of the ArsA ATPase. *J. Biol. Chem. 280*, 9921–9926.
23. Chung, C. T., Niemela, S. L., and Miller, R. H. (1989) One-step preparation of competent *Escherichia coli*: transformation and storage of bacterial cells in the same solution. *Proc. Natl. Acad. Sci. U.S.A. 86*, 2172–2175.
24. Kuroda, M., Bhattacharjee, H., and Rosen, B. P. (1998) Arsenical pumps in prokaryotes and eukaryotes. *Methods Enzymol. 292*, 82–97.
25. Hsu, C. M., and Rosen, B. P. (1989) Characterization of the catalytic subunit of an anion pump. *J. Biol. Chem. 264*, 17349–17354.
26. Ruan, X., Bhattacharjee, H., and Rosen, B. P. (2006) Cys-113 and Cys-422 form a high affinity metalloid binding site in the ArsA ATPase. *J. Biol. Chem. 281*, 9925–9934.
27. Walmsley, A. R., Zhou, T., Borges-Walmsley, M. I., and Rosen, B. P. (1999) The ATPase mechanism of ArsA, the catalytic subunit of the arsenite pump. *J. Biol. Chem. 274*, 16153–16161.
28. Walmsley, A. R., Zhou, T., Borges-Walmsley, M. I., and Rosen, B. P. (2001) Antimonite regulation of the ATPase activity of ArsA, the catalytic subunit of the arsenical pump. *Biochem. J. 360*, 589–597.
29. Walmsley, A. R., Zhou, T., Borges-Walmsley, M. I., and Rosen, B. P. (2001) A kinetic model for the action of a resistance efflux pump. *J. Biol. Chem. 276*, 6378–6391.
30. Zhou, T., Liu, S., and Rosen, B. P. (1995) Interaction of substrate and effector binding sites in the ArsA ATPase. *Biochemistry 34*, 13622–13626.
31. Zhou, T., and Rosen, B. P. (1997) Tryptophan fluorescence reports nucleotide-induced conformational changes in a domain of the ArsA ATPase. *J. Biol. Chem. 272*, 19731–19737.

32. Kaur, P. (1999) The anion-stimulated ATPase ArsA shows unisite and multisite catalytic activity. *J. Biol. Chem. 274*, 25849–25854.
33. Ramaswamy, S., and Kaur, P. (1998) Nucleotide binding to the C-terminal nucleotide binding domain of ArsA: studies with an ATP analogue, 5′-*p*-fluorosulfonylbenzoyladenosine. *J. Biol. Chem. 273*, 9243–9248.
34. Bhattacharjee, H., Choudhury, R., and Rosen, B. P. (2008) Role of conserved aspartates in the ArsA ATPase. *Biochemistry 47*, 7218–7227.
35. Emsley, P., and Cowtan, K. (2004) Coot: model-building tools for molecular graphics. *Acta Crystallogr., Sect. D: Biol. Crystallogr. 60*, 2126–2132.